Applied Catalysis B: Environmental 91 (2009) 406–415

Contents lists available at ScienceDirect

Applied Catalysis B: Environmental

journal homepage: www.elsevier.com/locate/apcatb

Performance of K-promoted hydrotalcite-derived CoMgAlO catalysts used for soot combustion, NOx storage and simultaneous soot–NOx removal

Qian Li [a], Ming Meng [a,*], Noritatsu Tsubaki [b], Xingang Li [a], Zhaoqiang Li [a], Yaning Xie [c], Tiandou Hu [c], Jing Zhang [c]

[a] Tianjin Key Laboratory of Applied Catalysis Science and Engineering, Department of Catalysis Science & Technology, School of Chemical Engineering & Technology, Tianjin University, Tianjin 300072, PR China
[b] Department of Applied Chemistry, School of Engineering, University of Toyama, Gofuku 3190, Toyama city, Toyama 930-8555, Japan
[c] Institute of High Energy Physics, Chinese Academy of Sciences, Beijing 100049, PR China

ARTICLE INFO

Article history:
Received 29 January 2009
Received in revised form 24 May 2009
Accepted 11 June 2009
Available online 18 June 2009

Keywords:
Soot
NOx
Hydrotalcite-derived CoMgAlO catalysts
Potassium
Calcination temperature

ABSTRACT

A series of K-promoted hydrotalcite-derived CoMgAlO catalysts were synthesized by coprecipitation. Their catalytic performance for soot combustion, NOx storage and simultaneous soot–NOx removal was evaluated, respectively. The techniques of TG/DTA, BET, XRD, EXAFS, XPS and *in situ* DRIFTS were employed for catalyst characterization. When K is added to the catalyst CoMgAlO, soot combustion is largely accelerated, with the temperature (T_m) for maximum soot conversion lowered by at least 50 °C. Moreover, the NOx reduction by soot over the catalysts calcined at 500–700 °C is also facilitated. The K-containing catalyst calcined at 600 °C shows not only the highest soot combustion rate, but also the maximum NOx reduction percentage of 32%, which is attributed to its high surface K/Co atomic ratio and the strong interaction between K and Co. *In situ* DRIFTS results reveal that NO is readily oxidized to NO_2 and stored as nitrates over K-promoted catalysts, which could be reduced by soot more efficiently. Based on these investigations, a reaction pathway for soot combustion, NOx storage and simultaneous soot–NOx removal is proposed.

1. Introduction

Recently, diesel engines are preferred for heavy-duty implements and light-duty trucks due to their high economy, high durability and low maintenance costs [1]. The high compression ratios and relatively high O_2 concentrations in the diesel combustion chambers are responsible for better fuel efficiency and lower emission of carbon oxides and hydrocarbon as compared with the gasoline engines [2]. However, a lot of nitrogen oxides (NOx) and soot particles are simultaneously formed under such condition, which can cause serious environmental and health problems. Since the simultaneous removal of NOx and soot particles cannot be accomplished by engine modifications alone, catalytic techniques for reducing the emission of both kinds of the harmful substances must be developed.

Simultaneous removal of soot and NOx was first proposed by Yoshida et al., who found CuO-based oxides effective for this catalytic process [3]. Afterwards, precious metals [4,5], zeolites [6], perovskite-related oxides [7–11] and spinel phases [12–14] were also applied to this reaction. Recently, the catalysts promoted by K have received more and more attention for soot combustion and NOx storage/reduction due to their high mobility and strong basicity [15–19]. Besides, calcined hydrotalcite-like compounds (HTlcs) containing transition metals also show novel redox properties, which have been applied to the catalytic removal of NOx and SOx [20–26], as well as the oxidation reactions [27–29]. Their redox performance strongly depends on the metal species, metal contents and catalyst calcination temperature. Wang et al. [30] have ever investigated the catalytic performance of hydrotalcite-derived Co–Al mixed oxides used for simultaneous removal of soot and NOx. They found that both the activity for soot oxidation and the selectivity to N_2 of the catalyst calcined at 800 °C are higher than those of the catalyst calcined at 500 °C, which is attributed to the improvement of redox properties. Promoted by potassium, hydrotalcite-derived catalysts show better performance for soot combustion and NOx storage/reduction. Zhang et al. found that KNO_3 or K_2CO_3 supported Mg–Al hydrotalcite-derived mixed oxides possess high catalytic activity for soot combustion [31]. Moreover, Takahashi et al. found that the NOx storage ability of the potassium-based NOx storage material could be improved at high temperature by using hydrotalcite-derived $MgAl_2O_4$ spinel as support [32]. So what about the catalytic performance of K-containing hydrotalcite-derived compounds for the simultaneous soot combustion and NOx storage/reduction?

* Corresponding author. Tel.: +86 022 2789 2275; fax: +86 022 2789 2275.
E-mail address: mengm@tju.edu.cn (M. Meng).

0926-3373/$ – see front matter © 2009 Elsevier B.V. All rights reserved.
doi:10.1016/j.apcatb.2009.06.007

In our previous work [33], the effect of K loading on the performance of hydrotalcite-derived CoMgAlO catalysts was studied carefully. We found that when the weight loading of K reaches 4.5%, the prominent enhancement effect is observed. However, there are still some unsolved problems, such as the essence of the promotional effect of potassium and the influence of calcination temperature on the active phases, as well as the mechanisms of soot combustion and NOx storage/reduction. For continuity, the purpose of this study is mainly to investigate the function of K, the effect of calcination temperature on the structures and properties of K-promoted CoMgAlO catalysts used for soot combustion, NOx storage and the simultaneous removal of soot and NOx. On the basis of *in situ* DRIFTS results, potential reaction mechanisms are proposed and discussed in detail.

2. Experimental

2.1. Catalyst preparation

The HTlc $Co_{2.5}Mg_{0.5}$/Al was prepared using pH-constant coprecipitation by adding mixed salt solution and mixed basic solution dropwise into distilled water simultaneously under vigorous mechanical stirring. The mixed salt solution consists of metal nitrates of $Co(NO_3)_2{\cdot}6H_2O$, $Mg(NO_3)_2{\cdot}6H_2O$ and $Al(NO_3)_3{\cdot}9H_2O$ with the designed molar ratio. The mixed basic solution contains NaOH and Na_2CO_3 with $[OH^-] = 2.0$ M and $[OH^-]/[CO_3^{2-}] = 16$. Precipitates were kept in suspension at 60 °C under stirring for 4 h, then filtered and thoroughly washed with distilled water. After the cake was dried at 70 °C for 12 h and at 120 °C overnight, the precursor of HTlc was calcined at 500, 600, 700 or 800 °C for 4 h to get the desired catalysts CoMgAl-oxide (CMAO), denoted as CMAO-T, where T represents the calcination temperature.

Catalysts promoted by potassium were prepared by impregnation using KNO_3 as the precursor. Powder of CMAO-T was added into the solution of KNO_3 under stirring. Then, the slurry was dried at 120 °C and finally calcined at 500 °C for 2 h. The weight loading of K in all promoted catalysts is 4.5 wt.%. The final catalysts are denoted as 4.5%K/CMAO-T.

2.2. Catalyst characterization

The crystal structures of fresh samples were determined by X-ray diffraction measurement on an X′pert Pro rotatory diffractometer operating at 30 mA and 45 kV using Co Kα as radiation source (λ = 0.1790 nm). The data of 2θ from 10° to 100° were collected with the stepsize of 0.033°.

Surface area, pore volume and pore size distribution were measured by nitrogen adsorption/desorption at 77 K using a Quadrasorb SI instrument. The samples were degassed at 350 °C for 10 h prior to the adsorption experiments. The surface area (S_{BET}) was determined by BET method in 0–0.3 partial pressure range and the pore size distribution was determined by Barrett–Joyner–Halenda (BJH) method from the desorption branch of the isotherm.

H_2-TPR measurements were performed on a Thermo-Finnigan TPDRO 1100 instrument equipped with a thermal conductivity detector (TCD). Before detection by the TCD, the gas was purified by a trap containing CaO + NaOH materials in order to remove H_2O and CO_2. A heating rate of 10 °C/min and a gas flow rate of 20 mL/min were used. The reducing gas was 5 vol.% H_2 balanced by pure N_2. Each time, the quartz tube reactor was loaded with 20 mg sample in powder form and heated from room temperature to 900 °C.

X-ray photoelectron spectra (XPS) were recorded with a PHI-1600 ESCA spectrometer using Mg Kα radiation (1253.6 eV). The base pressure was 5×10^{-8} Pa. The binding energies were calibrated using C 1s peak of contaminant carbon (BE = 284.6 eV) as standard, and quoted with a precision of ±0.2 eV. The surface composition of the samples was calculated in terms of atomic ratios.

Extended X-ray absorption fine structure (EXAFS) measurements were carried out on the 1W1B beamline of Beijing Synchrotron Radiation Facility (BSRF) operating at about 120 mA and 2.5 GeV. The absorption spectra of Co K-edge of the samples and the reference compounds Co_3O_4 and $CoAl_2O_4$ were recorded at room temperature. A Si(1 1 1) double crystal monochromator was used to reduce the harmonic content of the monochrome beam. The back-subtracted EXAFS function was converted into k space and weighted by k^3 in order to compensate for the diminishing amplitude due to the decay of the photoelectron wave. The Fourier transforming of the k^3-weighted EXAFS data was performed in the range of k = 3–14 A^{-1} with a Hanning function window.

In situ DRIFTS experiments were performed on a Nicolet Nexus spectrometer. The spectrometer was equipped with a MCT detector cooled by liquid nitrogen and a heating chamber allowing samples to be heated up to 600 °C. The DRIFTS spectra were recorded against a background spectrum of the sample purified just prior to introducing the adsorbates. In each run, about 15 mg of the sample in powder form was used. The NOx adsorption was carried out in order to reveal the NOx storage mechanism. The sample was pretreated under 5 vol.% O_2/He at 100 °C for 30 min, and then exposed to a flow of 400 ppm NO + 2 vol.% O_2 + balance He. The spectra of NOx adsorption from 100 to 600 °C at intervals of 50 °C were recorded with a spectral resolution of 4 cm^{-1}.

2.3. Activity measurement

For soot combustion, the catalytic activity of the prepared samples was evaluated by TG/DTA technique using Printex-U soot purchased from Degussa Company. Before measurements, the soot was mixed with the catalyst in a weight ratio of 1:20 in an agate mortar for 30 min to obtain a tight contact. Then the mixture was loaded to the sample chamber and heated from room temperature to 800 °C at a rate of 10 °C/min in air flow. By comparing characteristic temperatures of TG/DTA profiles, catalytic activity of samples was evaluated. In this work, soot ignition temperature (denoted as T_i), the temperature of the maximum rate of soot conversion (denoted as T_m) and complete conversion temperature of soot (denoted as T_f) were used to evaluate the performance of the catalysts. Besides, TG/DTA experiments were also carried out to study the reactivity of soot exposing to different atmospheres, including pure N_2, 10 vol.% O_2 + balance N_2, 20 vol.% O_2 + balance N_2, 400 ppm NO + balance N_2, and 400 ppm NO + 10 vol.% O_2 + balance N_2.

For NOx storage and removal, experiments were carried out in a continuous fixed-bed reactor under atmosphere pressure, with the gas mixture containing 400 ppm NO, 10 vol.% O_2 and N_2 for balance. The granular sample (40–60 mesh, 0.2 g) of soot/catalyst mixture was fixed in a quartz tube (i.d. = 8 mm) by packing quartz wool at the end of the bed. Gaseous mixtures were fed to the sample at 400 mL/min and the sample was heated from 100 to 700 °C at a constant rate of 10 °C/min. An on-line NO–NO_2–NOx analyzer (Thermo Scientific) was used to measure the NOx concentration in the effluent gas.

3. Results and discussion

3.1. Characterization of the catalysts

Fig. 1(a) displays the XRD patterns of the hydrotalcite-derived catalysts calcined at different temperatures. After calcined at 500 °C, the precursor $Co_{2.5}Mg_{0.5}$Al-HT (CMA-HT) [34,35] has been transformed into $Co_{2.5}Mg_{0.5}$Al-oxide (CMAO), which mainly

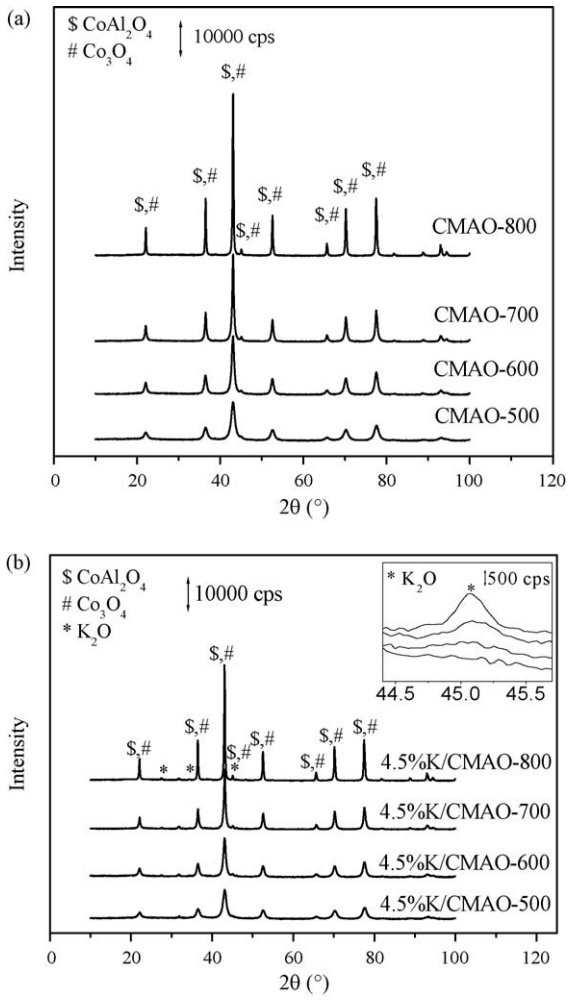

Fig. 1. XRD patterns of the catalysts calcined at different temperatures: (a) CMAO-T; (b) 4.5%K/CMAO-T.

consists of Co-related phases (Co_3O_4 and/or $CoAl_2O_4$), characterized by a group of diffraction peaks at ~22.1°, 36.6°, 43.1°, 52.7°, 65.7°, 70.3° and 77.6°. These peaks become sharper and stronger as the calcination temperature increases. No diffracted peaks for Mg-related phases are detected, suggesting that it is in non-crystalline state or is present as a part of the aluminum spinel phase or CoMg solid solution. It is noticeable that the catalysts calcined at 700 or 800 °C display light blue color, suggesting the existence of $CoAl_2O_4$ or $CoAl_2O_4$-like spinel phases. However, such spinels could not be the main phases since the content of Al in $Co_{2.5}Mg_{0.5}Al$-oxide is limited.

After the addition of K, no peak shifts of Co-related phases are observed as shown in Fig. 1(b). The absence of diffracted peaks of K_2O phases in 4.5%K/CMAO-500 indicates that K species are highly dispersed in this catalyst. However, as the calcination temperature is elevated to 600 °C or higher, K_2O phase is detected, characterized by the peaks appearing at ~27.6°, 34.5° and 45.1°. These peaks become stronger with the increase of calcination temperature, suggesting the growth of K_2O crystallites.

From above XRD results, it is hard to distinguish the main existing Co phase in these catalysts. Thus, EXAFS measurement was performed. The radial structure functions (RSFs) of Co K-edge of the reference compounds (Co_3O_4 and $CoAl_2O_4$) and catalysts CMAO-600 and 4.5%K/CMAO-T are presented in Fig. 2. It is known that the Co environment in Co_3O_4 corresponds to a spinel atomic arrangement with Co^{2+} and Co^{3+} ions located in tetrahedron (Td) and octahedron (Oh) coordination. Averagely, each Co atom coordinates

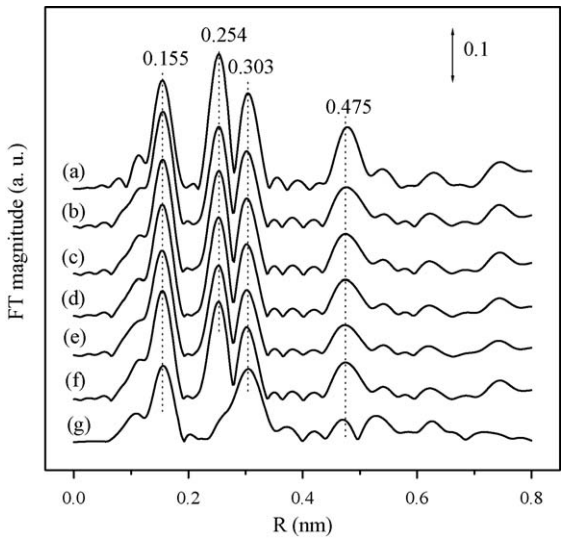

Fig. 2. Co K-edge radial structure functions of the catalysts and reference compounds: (a) Co_3O_4; (b) 4.5%K/CMAO-800; (c) 4.5%K/CMAO-700; (d) 4.5%K/CMAO-600; (e) 4.5%K/CMAO-500; (f) CMAO-600; (g) $CoAl_2O_4$.

with 5.3 O at 0.191 nm (first shell), 4 Co at 0.285 nm (second shell) and 8 Co at 0.336 nm (third shell) [36,37]. Therefore, in Fig. 2 the first three peaks in the RSF of Co_3O_4 at 0.155, 0.254, 0.303 nm (not corrected by phase scattering shift) can be assigned to the above three coordination shells. The fourth peak at 0.475 nm corresponds to higher Co–Co coordination shell. In $CoAl_2O_4$, all Co^{2+} ions possess tetrahedron (Td) symmetry, each Co coordinates with 4 O at 0.195 nm and 12 Co at 0.336 nm [38], corresponding to the first two peaks at 0.155 and 0.301 nm in the RSF of $CoAl_2O_4$ (not corrected by phase scattering shift), as displayed in Fig. 2. It can be easily found that the RSFs of the samples are similar to that of Co_3O_4, indicating that most cobalt exists as Co_3O_4 phase. With respect to the peak intensity, it can be clearly seen that the high coordination peaks are in the order of Co_3O_4 > 4.5%K/CMAO-800 ≈ 4.5%K/CMAO-700 > 4.5%K/CMAO-600 > 4.5%K/CMAO-500. Generally, the intensity of high coordination peaks provides a direct indication of the crystallization degree of the corresponding metal or oxides [39,40]. So, it can be deduced that the crystallization degree of Co_3O_4 is increased with the elevation of calcination temperature, which is in consistent with XRD results above. In comparison of the RSFs of Co K-edge of the samples CMAO-600 and 4.5%K/CMAO-600, no big change is found, suggesting little change in the average crystallite size of Co_3O_4 phase after the addition of K.

Table 1 shows the texture data of CMA-H, CMAO-T catalysts, as well as the K-promoted ones. The sample CMAO-500 possesses much larger specific surface area than the hydrotalcite-like precursor CoMgAl-H, resulted from the lost of inter-layer water molecules and nitrate anions during the calcination of the precursor [41,42]. However, after calcination at higher temperatures than 500 °C, an obvious decrease in surface area and pore volume can be observed. As analyzed in XRD and EXAFS, most cobalt in CMAO-T exists as Co_3O_4 phase. So, a rough estimation on the crystallite size of Co_3O_4 was performed based on the line broadening of the $d_{1\,1\,1}$ reflection of Co_3O_4 in Fig. 1 by using Scherrer equation. The results are also listed in Table 1. It can be seen that the crystallite size of Co_3O_4 increases remarkably with the elevation of calcination temperature. When K is added to CMAO-T, the surface areas of these samples decrease to some extent, which is possibly due to the partial pore blocking by the introduction of K. Compared with the K-free catalysts calcined at the same calcination temperature, it is found that the crystallite size of Co_3O_4 in K-promoted catalysts nearly keep unchanged, regardless of the decrease of surface areas.

Table 1
Texture data and Co_3O_4 crystallite size of the catalysts and CMA-H precursor.

Sample	BET surface area (m^2/g)	Pore volume (mL/g)	Crystallite size (nm)[a]
CoMgAl-H	71	0.26	–
CMAO-500	105	0.35	7
CMAO-600	63	0.32	11
CMAO-700	57	0.26	15
CMAO-800	24	0.17	44
4.5%K/CMAO-500	80	0.28	7
4.5%K/CMAO-600	49	0.21	12
4.5%K/CMAO-700	40	0.19	16
4.5%K/CMAO-800	17	0.12	44

[a] Calculated from the line broadening of the $d_{1\,1\,1}$ reflection of Co_3O_4 using Scherrer equation.

To investigate the redox properties of the catalysts, H_2-TPR measurement was performed. The results are presented in Fig. 3. All the profiles of CMAO-T catalysts, as seen in Fig. 3(a), display two reduction regions, one between 200 and 500 °C and the other above 500 °C. The former can be attributed to the reduction of Co^{3+} to Co^{2+} dispersed in the Co_3O_4 phase [41], while the latter can be assigned to the reduction of Co^{2+}-related species [43]. When K is added to the catalyst CMAO-T, a new reduction peak below 350 °C arises in the TPR profile, as seen in Fig. 3(b), suggesting that a new phase is formed in the K-promoted samples. From the area of the region below 500 °C, it can be seen that the amounts of consumed H_2 obviously increase, as compared with those of the unpromoted catalysts. These results suggest that the strong interaction between K and Mg (Al) species, such as Mg–Al spinel and CoMg solid solution, facilitates the release of partial cobalt species from Co_3O_4, $CoAl_2O_4$ and CoMg solid solution in CMAO-T, enhancing the formation of a new K–Co–O interaction phase with higher reducibility. Additionally, as the calcination temperature increases, all the splitted peaks shift to higher temperatures, indicating that the reducibility of Co^{3+} to Co^{2+} in the Co_3O_4 crystallites becomes more difficult. Surprisingly, the peak around 720 °C seems unsensitive to the calcination temperature, attributing to reduction of the inactive Co^{2+}-related species.

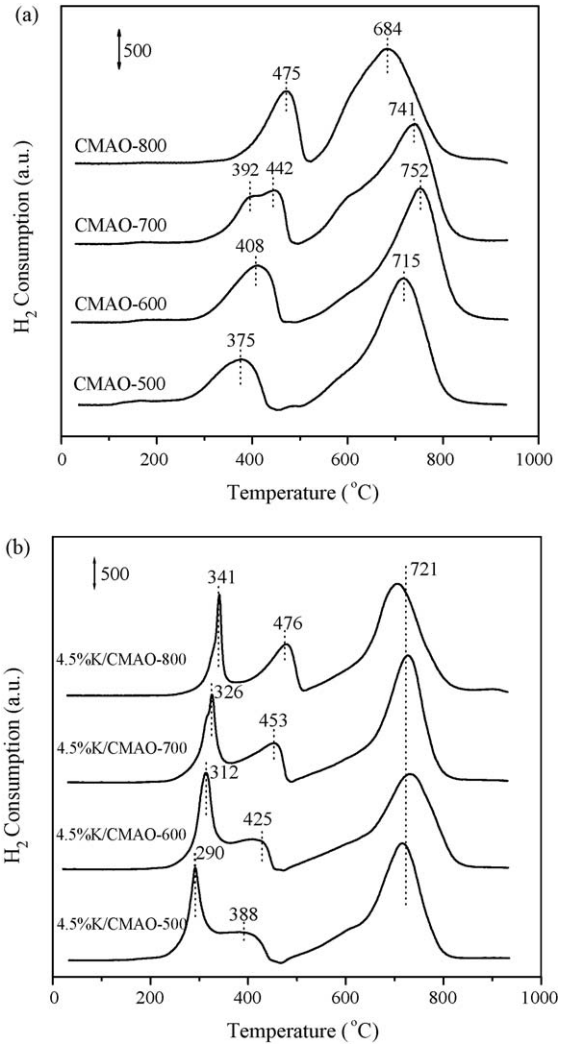

Fig. 3. H_2-TPR profiles of the catalysts: (a) CMAO-T; (b) 4.5%K/CMAO-T.

The chemical state and the relative proportion of the elements on the surface of the catalysts were studied by XPS technique, as listed in Table 2. The results show that the content of surface Co tends to decrease over CMAO-T catalysts with the increase of calcination temperature from 500 to 700 °C. After calcined at 800 °C, a slight increase of surface Co content is observed. The addition of K to CMAO-T makes the percentage of surface Co decrease to some extent with the catalyst 4.5%K/CMAO-700 as an exception. Similarly, for the surface K/Co atomic ratio, sample 4.5%K/CMAO-700 is also an exception, which possesses much lower surface K/Co atomic ratio than other three samples. Normally, high temperature calcination will lead to the sintering of cobalt phases, decreasing the surface Co content, as observed for the K-free samples, meanwhile, more potassium will enter the matrix of CMAO phases, decreasing the surface K content, as observed for the K-promoted ones. The K/Co atomic ratio is determined by the both factors of the above. It is noticeable that the surface K content of the sample 4.5%K/CMAO-800 is a little larger than that of 4.5%K/CMAO-700, which is tightly related to the serious sintering of 4.5%K/CMAO-800, as reflected by its much lower surface area (17 m^2/g). At the high temperature of 800 °C, the sintering of CMAO phases facilitates the migration of potassium ions from bulk to surface, resulting in the increase of surface K/Co atomic ratio.

3.2. Catalytic soot combustion over CMAO-T and 4.5%K/CMAO-T catalysts

The soot combustion activity in the atmosphere of 400 ppm NO and 10% O_2 balanced by N_2 over K-free CMAO-T catalysts was evaluated by TG-DTA technique, as shown in Fig. 4(a). On CMAO-500, the soot oxidation starts from 300 °C and ends at ~500 °C. With the increase of calcination temperature, DTG peaks of soot combustion shift to higher temperatures. Compared with CMAO-500, the temperature T_m for the catalyst calcined at 800 °C increases from 422 to 472 °C and the region for ΔT ($T_f - T_i$) is also broadened, attributing to the lowered combustion rate.

For K-promoted catalysts calcined at different temperatures, their soot combustion performances are presented in Fig. 4(b). The temperature T_m for maximum soot conversion over these catalysts

Table 2
Surface atomic percentages and K/M (M = O, Al, Co, Mg) atomic ratios for the catalysts CMAO-T and 4.5%K/CMAO-T from XPS measurement.

Sample	O 1s (%)	Al 2p (%)	Co 2p (%)	Mg 2p (%)	K 2p (%)	K/O	K/Al	K/Co	K/Mg
CMAO-500	66.1	13.1	12.0	8.9	–	–	–	–	–
CMAO-600	65.7	15.2	9.0	10.1	–	–	–	–	–
CMAO-700	67.7	15.9	6.4	9.7	–	–	–	–	–
CMAO-800	65.1	16.6	7.4	10.7	–	–	–	–	–
4.5%K/CMAO-500	64.4	11.0	11.1	11.0	2.5	0.039	0.227	0.225	0.227
4.5%K/CMAO-600	67.6	11.9	7.2	10.8	2.2	0.032	0.185	0.306	0.204
4.5%K/CMAO-700	66.7	15.3	7.3	9.3	1.3	0.019	0.085	0.178	0.140
4.5%K/CMAO-800	67.7	19.1	4.8	6.4	1.6	0.024	0.084	0.333	0.250

are at least 50 °C lower than those over K-free catalysts. Moreover, after the addition of K, much higher oxidation rates are achieved, as reflected by the much sharper and narrower peaks. Although as the calcination temperature increases, the temperature of the maximum rate of soot combustion (T_m) at ~371 °C changes very little, the average soot oxidation rates in the region of ΔT ($T_f - T_i$) over different catalysts are obviously different, which are 57.9, 70.1, 57.1, 51.5 $\mu g\ s^{-1}\ g^{-1}$ catalyst, corresponding to the catalysts calcined at 500, 600, 700 and 800 °C, respectively. Combining with these factors, the catalytic soot combustion activity over K-containing samples follows the order: 4.5%K/CMAO-600 > 4.5%K/CMAO-500 ≈ 4.5%K/CMAO-700 > 4.5%K/CMAO-800. Such sequence is not the same as that for the surface areas of the samples. Moreover, it is also hard to be interpreted from the view of redox properties based on H_2-TPR results. So, other aspects should be considered to figure out the reason that why the sample 4.5%K/CMAO-600 is the most active one among all the catalysts? It is worth noting that from the XPS data, it can be seen that the surface K/Co atomic ratio decreases in the following order: 4.5%K/CMAO-800 > 4.5%K/CMAO-600 > 4.5%K/CMAO-500 > 4.5%K/CMAO-700, which is in accordance with the activity order for the catalysts calcined at lower temperatures (500–700 °C). Therefore, surface K/Co atomic ratio is thought to be an important factor for soot combustion over these catalysts. However, the amount of surface Co sites is also very important, for sample 4.5%K/CMAO-800, too low surface area and too low content of surface Co mean much less active sites, which determines its worst performance for soot combustion.

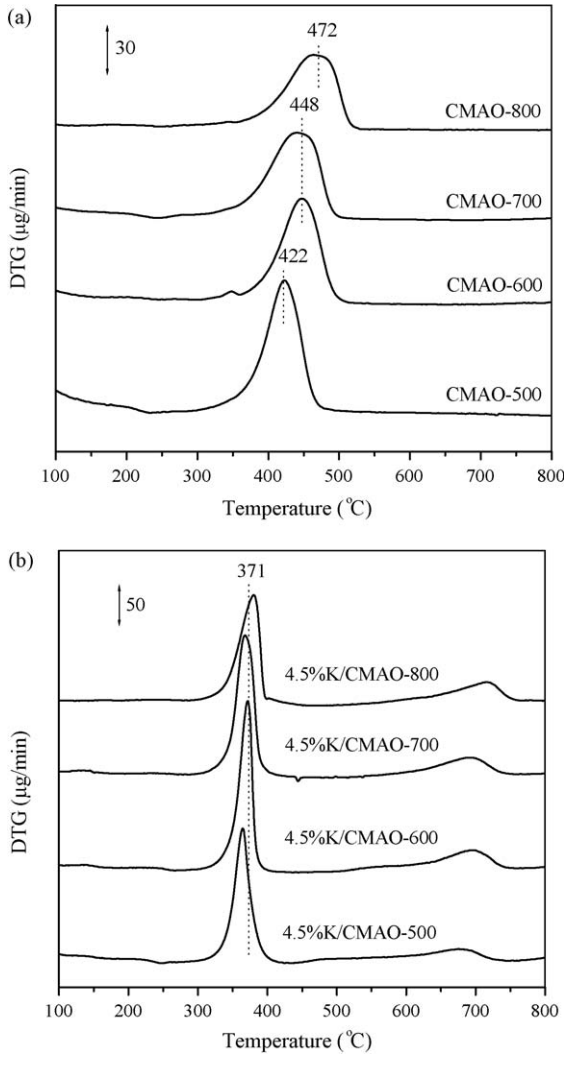

Fig. 4. DTG profiles of soot combustion in the atmosphere of 400 ppm NO + 10 vol.% O_2 balanced by N_2 over different catalysts: (a) CMAO-T; (b) 4.5%K/CMAO-T.

In order to investigate the promotional effects of K on soot combustion performance of the catalysts, soot combustion over CMAO-T and 4.5%K/CMAO-T catalysts in N_2 atmosphere was also performed, the results of which are displayed in Fig. 5. In this case, the soot oxidation activity reflects the reducibility of the samples. From Fig. 5(a), it can be found that over K-free catalysts, reducibility decreases as the calcination temperature increases. Addition of K has enhanced the reducibility of the samples, as shown in Fig. 5(b). Moreover, the DTG peaks of K-promoted samples appeared at much lower temperature of ~376 °C, regardless of the calcination temperature of the catalysts, which suggests the presence of new surface or bulk species possessing more active oxygen species. These results are in good agreement with H_2-TPR results. Additionally, considering the low melting points of K-related phases in the K-promoted samples, an additional promotion in soot combustion activity of the K-containing samples, due to the enhanced contact between soot and catalysts or the enhanced formation of carbonate intermediates [44,45], could not be neglected. All these factors determine that the K-promoted catalysts possess not only high activity for soot combustion, but also high thermal stability after calcined at high temperatures.

Since the active oxygen species play a crucial role in soot combustion, we want to know that how it works over those K-free and K-promoted samples? Thus, experiments under different atmospheres (N_2, N_2 + 10% O_2, N_2 + 20% O_2, N_2 + 400 ppm NO, N_2 + 10% O_2 + 400 ppm NO) were performed using the samples calcined at 600 °C as model catalysts, as shown in Fig. 6. The DTG profiles for soot combustion over CMAO-600 under different atmospheres are displayed in Fig. 6(a). It can be found that under pure N_2, considerable soot oxidation was not observed until 500 °C with extremely low oxidation rate. When O_2 was introduced, much lower characteristic temperature, as well as higher combustion rate was achieved. Further increase of O_2 concentration only affects the soot combustion rate. The addition of 400 ppm NO to pure N_2 could hardly enhance the soot combustion. However, introduction of 400 ppm NO to O_2-containing atmosphere can further lower the characteristic temperatures by ~30 °C for soot combustion, probably due to that NO can be oxidized to NO_2 over the

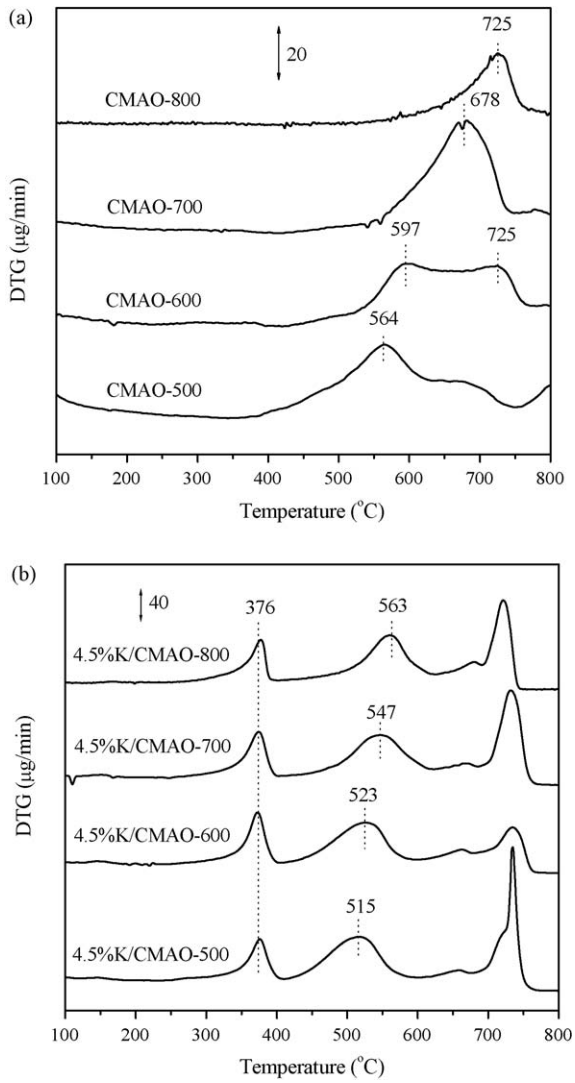

Fig. 5. DTG profiles of soot combustion in pure N_2 over the catalysts: (a) CMAO-T; (b) 4.5%K/CMAO-T.

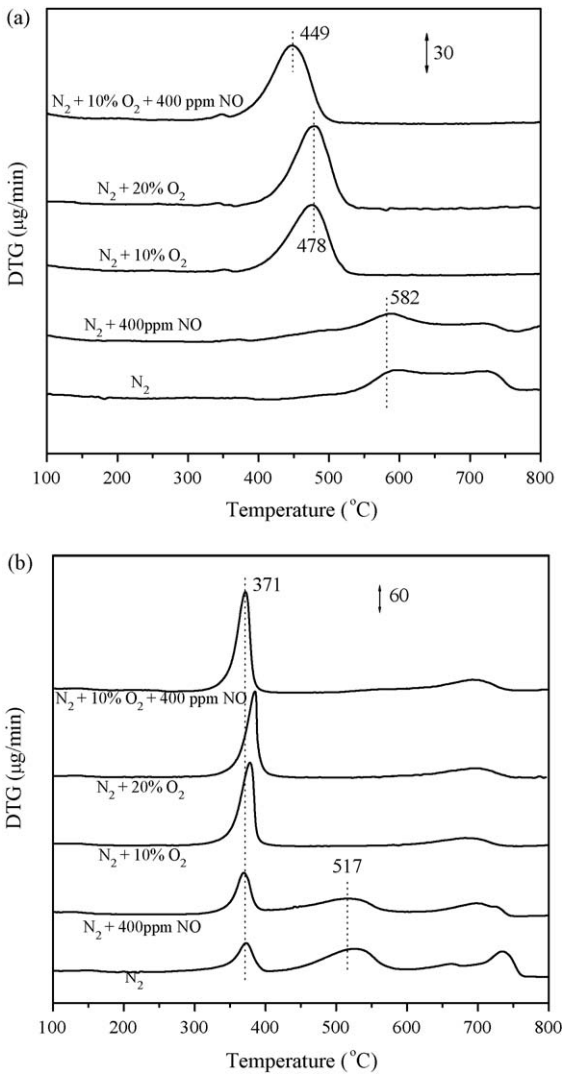

Fig. 6. DTG profiles of soot combustion in different atmospheres over (a) CMAO-600 and (b) 4.5%K/CMAO-600.

Co-containing catalysts, which is generally considered as the first and a crucial step during NOx storage [46–48]. Thus, the preformed NO_2 may serve as the stronger oxidant, facilitating the soot oxidation process.

Over the promoted catalyst 4.5%K/CMAO-600, different combustion performance can be observed, as displayed in Fig. 6(b). Although soot oxidation proceeds under different atmospheres, the first peaks appear at nearly the same position around 371 °C, indicating that dopant K can greatly enhance the reducibility of the samples. Under O_2-containing atmosphere, soot can be completely oxidized before 400 °C. Although the addition of 400 ppm NO could hardly change the characteristic temperatures, it does increase the oxidation rate remarkably, which is possibly due to the oxidation of NO to NO_2 and the consequent storage as potassium nitrite and/or nitrate. Such nitrite and nitrate species could oxidize the soot at much lower temperature. The formation of potassium nitrite and/or nitrate has been confirmed by *in situ* DRIFTS in the following section. In a word, in the presence of oxygen, the K-containing catalysts function in a different way from the K-free catalysts, on which the gaseous NO_2 molecules are formed and act as oxidant.

In order to investigate the difference of the catalytic performance over different samples, especially the essence of the promotional effect of K, experiments were carried out to study the interaction between K and Co in K-promoted samples. Thus, soot combustion activities in air over the Co-free catalyst, K-free catalyst and mechanically mixed K- and Co-containing samples were measured by TG-DTA technique. The K-free, Co-free and mechanically mixed samples were prepared by the same method, namely the pH-constant coprecipitation. According to the K/Co atomic ratio and K content in 4.5%K/CMAO-600, the mechanically mixed catalyst is composed of 73.9% of Co_3O_4-600 and 26.1% of 17.2%K/MgAlO-600. All the samples calcined at 600 °C were also used as the model catalysts, the soot combustion activity of the samples are shown in Fig. 7(a). It can be easily found that 4.5%K/CMAO-600 displays the best activity than the others, suggesting that the coexistence of K and Co and the strong interaction between them are the key factor to the high activity of K-promoted samples. For comparison, the same experiments were also carried out in N_2 atmosphere, displayed in Fig. 7(b). It can be seen that over 4.5%K/CMAO-600, the peak at 371 °C still exists even under inert gas (N_2), suggesting the formation of active lattice oxygen species in a new phase, which is consistent with TPR results (see Fig. 3(b)). However, no peak at this position was observed on K-free, Co-free or mechanically mixed K-containing and Co-containing samples. From these results, it is proposed that the essence of the strong interaction between K and Co lies in the formation of a new phase as K–Co–O species. Weaker Co–O bonds exist in this species compared to Co_3O_4, enhancing the reducibility of the K-promoted

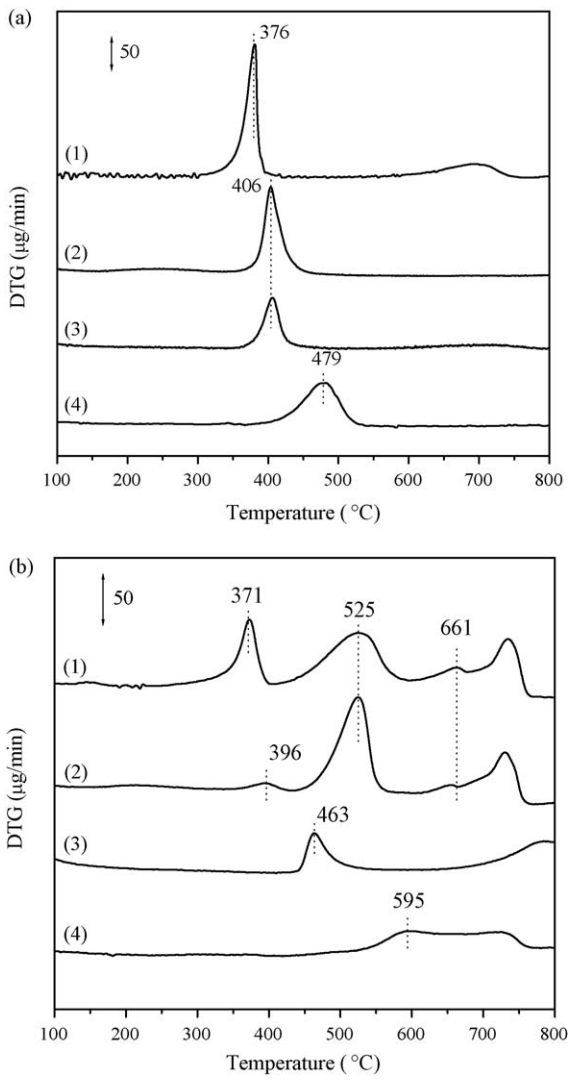

Fig. 7. DTG profiles of soot combustion over the Co-free catalyst, K-free catalyst and the samples containing Co and K in (a) air and (b) N_2. (1) 4.5%K/CoMgAlO-600, (2) Co_3O_4 + 17.2%K/MgAlO-600 (mechanically mixed), (3) 4.5%K/MgAlO-600, and (4) CoMgAlO-600.

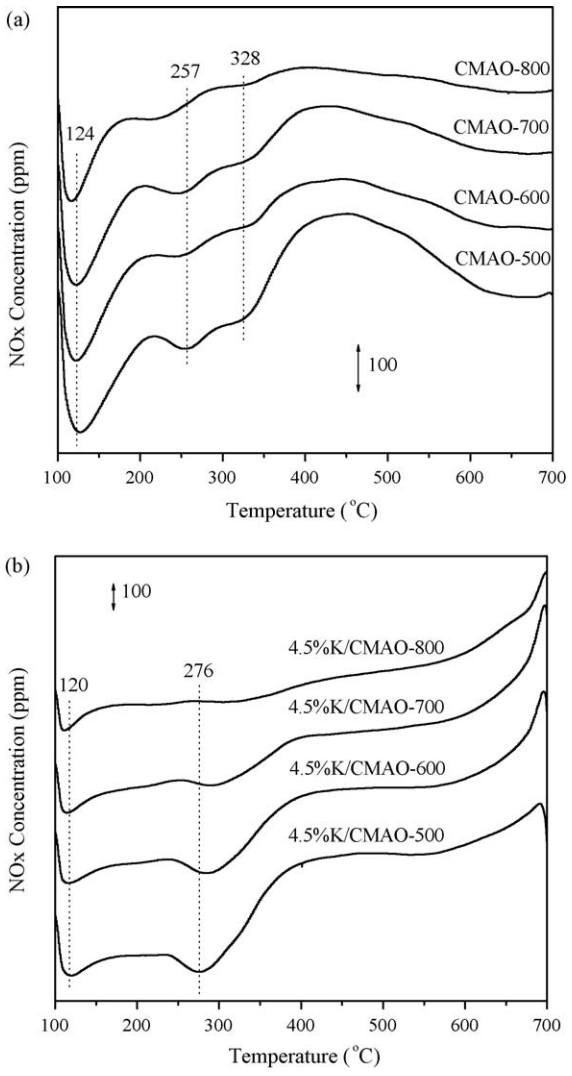

Fig. 8. NOx storage behaviors of the catalysts in the atmosphere of 400 ppm NO + 10 vol.% O_2 balanced by N_2: (a) CMAO-T; (b) 4.5%K/CMAO-T.

samples. Furthermore, it has been indicated that the surface atomic K/Co ratio has profound effects on the interaction of K with Co over the samples calcined at lower temperatures (500–700 °C). At higher calcination temperature of 800 °C, the sharp decrease of surface area and the amount of surface Co atoms is responsible for the activity decrease of the sample, even though it possesses the highest surface K/Co atomic ratio.

3.3. Catalytic NOx storage and reduction over CMAO-T and 4.5%K/CMAO-T catalysts

Fig. 8(a) displays the results of NOx storage capacity (NSC) on CMAO-T catalysts. The value of the starting point in each curve represents the NOx concentration in the gas feed and the point below and above this value means the occurrence of NOx sorption and desorption, respectively. The amounts of NOx uptake are calculated from the peak area of the absorption curves, which are listed in Table 3. It can be found that with the increase of calcination temperature, NSC decreases obviously. On the basis of the *in situ* DRIFTS results, the storage mechanism of NOx can be revealed. As seen in Fig. 9(a), in the first step between 100 and 200 °C, NOx is stored as nitrite species, characterized by the peak at 1248 cm^{-1} [49–53], and in the second step between 200 and 300 °C, NOx is stored as the chelating bidentate nitrate species, characterized by the peaks appearing at 1541 and 1275 cm^{-1}. Above 300 °C, NOx is still stored, but the gradual decomposition of nitrate species is observed with the formation of nitrite species, which is confirmed by the occurrence of the peaks at 1248 and 1471 cm^{-1}. Moreover, the peaks at 1590 and 1756 cm^{-1}, attributed to the adsorbed NO_2 species coming from the decomposition of nitrates or nitrites species, are clearly found. Simultaneously, the appearance of negative bands at 1520–1530 cm^{-1} is due to the decomposition of surface carbonates or

Table 3
NOx storage capacities of the catalysts CMAO-T and 4.5%K/CMAO-T.

Sample	NOx uptake (μmol/g catalyst)	Temperature ranges (°C)
CMAO-500	355	100–352
CMAO-600	206	100–335
CMAO-700	218	100–333
CMAO-800	152	100–273
4.5%K/CMAO-500	396	100–341
4.5%K/CMAO-600	323	100–348
4.5%K/CMAO-700	241	100–351
4.5%K/CMAO-800	168	100–386

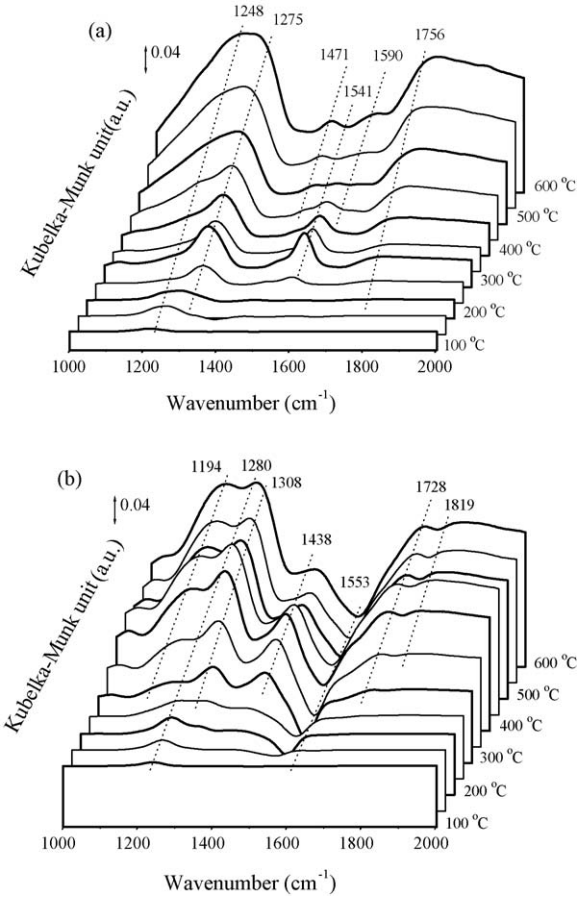

Fig. 9. *In situ* DRIFTS spectra of NOx sorption on the catalysts exposed to the atmosphere of 400 ppm NO + 2 vol.% O_2 balanced by helium: (a) CMAO-600; (b) 4.5%K/CMAO-600.

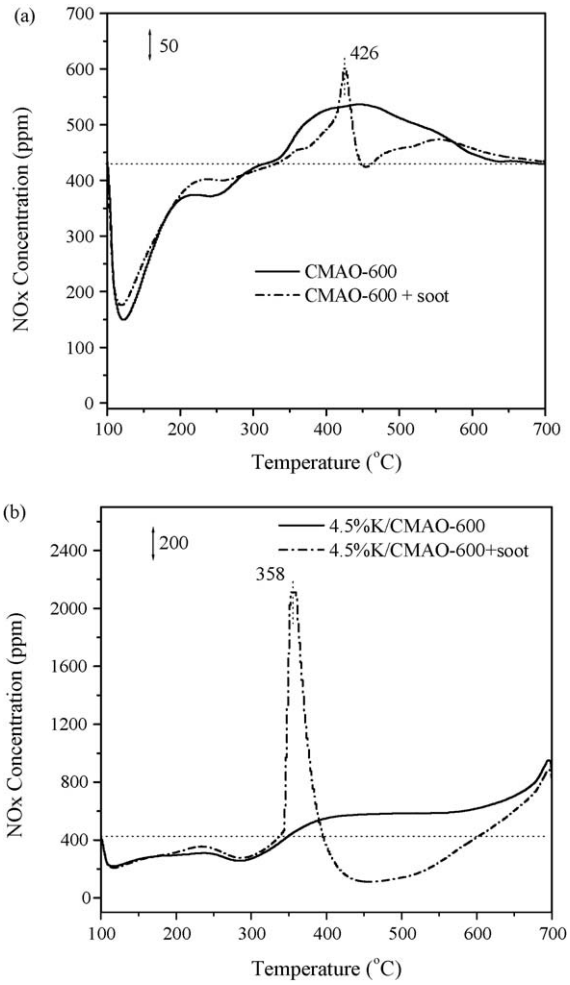

Fig. 10. Profiles of NOx storage in the atmosphere of 400 ppm NO + 10 vol.% O_2 balanced by N_2 over different catalysts mixed with or without soot: (a) CMAO-600 and soot/CMAO-600 mixture; (b) 4.5%K/CMAO-600 and 4.5%K/CMAO-600+soot mixture.

their transformation to nitrates or nitrites during the storage process.

Addition of K enhances the NSC of the samples to a great extent compared with the corresponding K-free catalysts, as seen in Fig. 8(b) and Table 3. As calcination temperature increases, decreased NSC was also observed. From the *in situ* DRIFTS results, as shown in Fig. 9(b), it can be found that all the profiles display two storage periods. In the first step between 100 and 200 °C, NOx is stored as the chelating bidentate nitrate species, corresponding to the bands at 1280 and 1553 cm^{-1}. In the second step between 200 and 350 °C, NOx is stored as the ionic nitrate species, corresponding to the bands at 1308 and 1438 cm^{-1}. At higher temperatures, a part of nitrate species decompose into nitrite species, characterized by the band at 1194 cm^{-1}. Moreover, adsorbed NO_2 species are formed as well, corresponding to the peaks at 1728 and 1819 cm^{-1}.

As described above, it can be concluded that the storage period below 200 °C is considered as the surface storage, which correlates well with the surface area of the catalysts, while the storage period at higher temperature region (200–350 °C) is attributed to the bulk storage. Dopant K enhances the NSC to a large degree, especially the bulk storage capacity. Previously, it has been proposed that the promotional effect of K lies in its strong interaction with cobalt species, inducing the formation of active lattice oxygen species in a new K–Co–O phase. Thus, in the storage condition, the introduced NO can be more easily oxidized by these as-formed active lattice oxygen species, resulting in the formation of NO_2 molecules in a more efficient way, which is generally considered as the first and a crucial step for NOx storage [46–48].

Fig. 10(a) exhibits the profiles of the NOx concentrations in effluent gas from the catalyst-bed loaded with CMAO-600 or soot/CMAO-600 mixture during a programmed process (10 °C/min) in a stream of 400 ppm NO, 10% O_2 and balance N_2. The dotted lines in the figure represent the NOx concentration in the gas feed, the points below and above this line mean the occurrence of NOx sorption/reduction and NOx desorption, respectively. The soot/CMAO-600 mixture and CMAO-600 show very similar NOx uptake performance at low temperature region (<290 °C), as seen in Fig. 10(a), but a noticeable difference exists at higher temperature region. Unlike the case of the CMAO-600 alone, the NOx concentration corresponding to soot/CMAO-600 mixture is lower than that for CMAO-600 in the region of 290–418 °C, suggesting the occurrence of reactions between NOx and soot. Afterwards, a sharp NOx desorption peak appears at 426 °C, just after the onset of the considerable soot combustion, referring to the DTG profiles of soot oxidation in Fig. 4(a), so, it is thought that the large amount of the released NOx comes from the decomposition of nitrate and/or nitrite, which is facilitated by the exotherm of soot combustion. Quickly, a sudden decrease of NOx concentration was observed, due to the reduction of NOx by the residual soot. Moreover, judging from observed areas below and above the dotted baseline for CMAO-600, the amounts of NOx sorption and desorption were almost the same. However, for soot/CMAO-600 mixture, the area below the dotted baseline is larger than that above it, corresponding to the

Table 4
NOx reduction percentages over soot/CMAO-T and soot/4.5%K/CMAO-T mixture.

Sample	NOx reduction (%)	Temperature range (°C)
CMAO-500	16	331–556
CMAO-600	9	284–573
CMAO-700	16	367–584
CMAO-800	10	264–626
4.5%K/CMAO-500	30	330–700
4.5%K/CMAO-600	32	336–700
4.5%K/CMAO-700	22	320–700
4.5%K/CMAO-800	5	342–700

amounts of 172 and 143 μmol NOx g^{-1} catalyst, respectively. This suggests that the partial adsorbed and/or stored NOx was reduced by soot during the experiments.

For K-promoted samples, the profiles are displayed in Fig. 10(b). Similarly, the 4.5%K/CMAO-600 and soot/4.5%K/CMAO-600 mixture show almost the same NOx uptake profile at low temperature region (<300 °C). However, when the temperature reaches 350 °C, a sharp and sudden peak for NOx desorption, arising from the decomposition of nitrate and/or nitrite species caused by the exothermic soot combustion is observed for soot/4.5%K/CMAO-600 mixture, followed by an obvious decrease in NOx concentration. From 400 to 700 °C, the NOx concentration for soot/4.5%K/CMAO-600 mixture is always lower than that for 4.5%K/CMAO-600. The areas below and above the dotted baseline for soot/4.5%K/CMAO-600 mixture correspond to the amounts of 498 and 437 μmol NOx g^{-1} catalyst, respectively, which are much larger than those for K-free samples, indicating that more NOx is stored and higher NOx removal efficiency is achieved after introduction of K.

To evaluate the catalytic performance for the simultaneous NOx–soot removal over CMAO-T and 4.5%K/CMAO-T, the NOx reduction percentages are calculated by comparing the amounts of desorbed NOx for the catalysts mixed with soot or not, the results of which are listed in Table 4. For K-free catalysts, CMAO-500 and CMAO-700 display much better activity than other two samples calcined at 600 and 800 °C. This could not be explained only on the basis of BET surface area. Actually, the reaction between NOx and soot is a oxidizing process, the soot oxidation activity by NOx of the catalysts is largely determined by the surface lattice oxygen mobility and the oxidation ability of the catalysts. From H_2-TPR results (see Fig. 3(a)), it is found that the sample CMAO-500 shows the best reducibility with the first reduction peak appearing at 375 °C. For the catalyst calcined at 700 °C, the first reduction peak spilts into two close peaks, one of which appears at 392 °C. While for the catalysts calcined at 600 and 800 °C, the first reduction peak appears at 408 and 475 °C, respectively, which are higher than those for CMAO-500 and CMAO-700, so that the later two catalysts show better activity for soot–NOx removal is intelligible. Previously, for soot combustion (see Fig. 4(a)), the catalysts CMAO-500 and CMAO-700 also show better activity than the other two according to the ignition temperature. In addition, the difference in active phases cannot be ignored. In Section 3.1, it is pointed out that the catalysts calcined at 700 or 800 °C display light blue color, which is the characteristic color of Co–Al spinel, therefore, the formation of $CoAl_2O_4$ or $CoAl_2O_4$-like spinels is confirmed. However, such spinels must be much less than Co_3O_4 because of the limited content of Al in $Co_{2.5}Mg_{0.5}Al$-oxide. It is indicated by our previous work [54] that the $CoAl_2O_4$ or $CoAl_2O_4$-like spinels are active phases for NOx selective reduction by hydrocarbons, in this work, the existence of a small amount of $CoAl_2O_4$ or $CoAl_2O_4$-like spinels is probably favorable to soot–NOx removal. At higher calcination temperature of 800 °C, the decrease of the NOx reduction percentage for the catalyst CMAO-800 should be mainly caused by the sintering of the active phases, such as

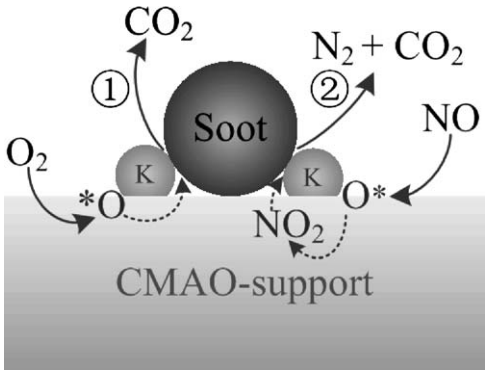

Fig. 11. Proposed reaction mechanism for simultaneous soot oxidation and NOx reduction over K-promoted catalysts.

Co_3O_4 and $CoAl_2O_4$ or $CoAl_2O_4$-like spinels, which is well reflected by the BET surface area, XRD and EXAFS results.

After the addition of K, the NOx reduction is remarkably increased except the sample calcined at 800 °C. Among the four samples, the sample 4.5%K/CMAO-600 shows the highest NOx reduction percentage, which is related to its high surface K/Co atomic ratio. When NO on the surface of the catalyst is oxidized to NO_2 by the active lattice oxygen species, NO_2 can react quickly with K species due to the strong interaction between K and Co species. Afterwards, this pre-formed nitrate species can be readily reduced by soot. For the sample calcined at 800 °C, the worst performance is observed, which is attributed to its much lower surface area and the smallest amount of surface Co atoms, though it has the highest surface K/Co atomic ratio.

Based on the above results and analysis, a mechanism scheme for the simultaneous removal of soot and NOx on the potassium promoted catalysts is proposed, as presented in Fig. 11. On the one hand, the strong interaction of surface K and Co species on CMAO-support induces the formation of the active oxygen species (denoted as O*) in a new K–Co–O phase, which will readily react with soot on the catalyst surface. Under O_2-containing atmosphere, this active oxygen species can be continuously provided by the filling up of gaseous O_2, ensuring continuous high soot combustion activity over the K-containing samples. On the other hand, NO molecules can be easily oxidized to NO_2 by the referred active oxygen species and then stored as nitrates on K species, which can be reduced by soot to give N_2 and CO_2.

4. Conclusions

For soot combustion, the activity of K-free catalysts decreases as the calcination temperature increases. Surprisingly, high catalytic performance could be maintained on K-promoted catalysts even at high calcination temperature of 800 °C. It is proposed that the strong interaction between K and Co induces the formation of the active oxygen species in a new K–Co–O phase, which readily reacts with soot on the catalyst surface. Continuous transfer of oxygen from gaseous phase to catalyst surface ensures the high soot combustion activity on the K-containing catalysts.

For NOx storage, the addition of K remarkably increases the NOx storage capacity compared with K-free catalysts. Meanwhile, the temperature ranges for NOx storage are broadened to some extent, attributed to more KNO_3 formation. With the elevation of calcination temperature, NOx uptake is reduced due to the sintering of the catalysts, reflected by the obvious decrease in surface area and surface Co content.

Simultaneous catalytic removal of soot and NOx can be achieved over the hydrotalcite-derived CoMgAlO catalysts in the temperature range of 300–700 °C. The catalysts calcined at 500 and

700 °C show better performance for NOx removal than those calcined at 600 and 800 °C. Both Co_3O_4 and $CoAl_2O_4$ or $CoAl_2O_4$-like spinels are active phases for NOx reduction by soot. Addition of 4.5 wt.% K to CoMgAlO catalyst is very effective on both soot combustion and NOx storage/reduction. The catalyst 4.5%K/CMAO calcined at 600 °C shows the best performance, not only for soot combustion but also for simultaneous soot–NOx removal. Over this catalyst, the NOx reduction percentage can reach as high as 32%.

Acknowledgements

This work is financially supported by the National Natural Science Foundation of China (No. 20876110, No. 20676097), the "863" Programs of the Ministry of Science and Technology of China (No. 2008AA06Z323, No. 2006AA06Z348) and the Program of New Century Excellent Talents in University of China (NCET-07-0599). The authors are also grateful to the Natural Science Foundation of Tianjin (No. 07JCYBJC15100), the Cheung Kong Scholar Program for Innovative Teams of the Ministry of Education (No. IRT0641) and the Program of Introducing Talents of Discipline to University of China (No. B06006).

References

[1] R.H. Hammerle, D.A. Ketcher, R.W. Horrocks, G. Lepperhoff, G. Húth-wohl, B. Lúers, SAE Paper 942043 (1994).
[2] J.C. Summers, S. Van Houtte, D. Psaras, Appl. Catal. B 10 (1996) 139.
[3] K. Yoshida, S. Makino, S. Sumiya, G. Muramatsu, R. Helferich, SAE Paper 892046 (1996).
[4] K. Matsuoka, H. Orikasa, Y. Itoh, P. Chambrion, A. Tomita, Appl. Catal. B 26 (2000) 89.
[5] A. Setiabudi, M. Makkee, J.A. Moulijn, Appl. Catal. B 42 (2003) 35.
[6] A. Fritz, V. Pitchon, Appl. Catal. B 13 (1997) 1.
[7] Y. Teraoka, K. Nakano, S. Kagawa, W.F. Shangguan, Appl. Catal. B 5 (1995) L181.
[8] Y. Teraoka, K. Nakano, W.F. Shangguan, S. Kagawa, Catal. Today 27 (1996) 107.
[9] Y. Teraoka, K. Kanada, S. Kagawa, Appl. Catal. B 34 (2001) 73.
[10] D. Fino, P. Fino, G. Saracco, V. Specchia, Appl. Catal. B 43 (2003) 243.
[11] J. Liu, Z. Zhao, C.M. Xu, A.J. Duan, Appl. Catal. B 78 (2008) 61.
[12] W.F. Shangguan, Y. Teraoka, S. Kagawa, Appl. Catal. B 8 (1996) 217.
[13] W.F. Shangguan, Y. Teraoka, S. Kagawa, Appl. Catal. B 12 (1997) 237.
[14] W.F. Shangguan, Y. Teraoka, S. Kagawa, Appl. Catal. B 16 (1998) 149.
[15] K. Krishna, M. Makkee, Catal. Today 114 (2006) 48.
[16] N. Nejar, M. Makkee, M.J. Illán-Gómez, Appl. Catal. B 75 (2007) 11.
[17] N. Nejar, M.J. Illán-Gómez, Appl. Catal. B 70 (2007) 261.
[18] N. Russo, S. Furfori, D. Fino, G. Saracco, V. Specchia, Appl. Catal. B 83 (2008) 85.
[19] L. Castoldi, R. Matarrese, L. Lietti, P. Forzatti, Appl. Catal. B (2009), doi:10.1016/j.apcatb.2009.03.022.
[20] A. Corma, A.E. Palomares, F. Rey, F. Márquez, J. Catal. 170 (1997) 140.
[21] L. Chmielarz, P. Kuśtrowski, A. Rafalska-Łasocha, D. Majda, R. Dziembaj, Appl. Catal. B 35 (2002) 195.
[22] J.J. Yu, Z. Jiang, L. Zhu, Z.P. Hao, Z.P. Xu, J. Phys. Chem. B 110 (2006) 4291.
[23] J.J. Yu, Y.X. Tao, C.C. Liu, Z.P. Hao, Z.P. Xu, Environ. Sci. Technol. 41 (2007) 1399.
[24] J. Pérez-Ramírez, J. Overeijnder, F. Kapteijn, J.A. Moulijn, Appl. Catal. B 23 (1999) 59.
[25] L. Obalová, K. Karásková, K. Jirátová, F. Kovanda, Appl. Catal. B (2009), doi:10.1016/j.apcatb.2009.03.002.
[26] H.K. Cheng, Y.Q. Huang, A.Q. Wang, L. Li, X.D. Wang, T. Zhang, Appl. Catal. B (2009), doi:10.1016/j.apcatb.2008.12.018.
[27] Z. Jiang, Z.P. Hao, J.J. Yu, H.X. Hou, C. Hu, J.X. Su, Catal. Lett. 99 (2005) 157.
[28] J.J. Yu, Z. Jiang, S.F. Kang, Z.P. Hao, Acta Phys. Chim. Sin. 20 (2004) 1459.
[29] A.F. Lucrédio, G. Jerkiewicz, E.M. Assaf, Appl. Catal. B 84 (2008) 106.
[30] Z.P. Wang, Z. Jiang, W.F. Shangguan, Catal. Commun. 8 (2007) 1659.
[31] Z.L. Zhang, Z.G. Mou, P.F. Yu, Y.X. Zhang, X.Z. Ni, Catal. Commun. 8 (2007) 1621.
[32] N. Takahashi, S. Matsunaga, T. Tanaka, H. Sobukawa, H. Shinjoh, Appl. Catal. B 77 (2007) 73.
[33] Q. Li, M. Meng, Z.Q. Zou, X.G. Li, Y.Q. Zha, J. Hazard. Mater. 161 (2009) 366.
[34] F. Cavani, F. Trifiró, A. Vaccari, Catal. Today 11 (1991) 173.
[35] P.S. Braterman, Z.P. Xu, F. Yarberry, in: K.A. Carrado, P.K. Dutta (Eds.), Handbook of Layered Materials, Marcel Dekker Inc., New York, 2004, p. 373.
[36] F. Morales, D. Grandjean, A. Mens, F.M.F. de Groot, B.M. Weckhuysen, J. Phys. Chem. B 110 (2006) 8626.
[37] J.Y. Luo, M. Meng, X. Li, X.G. Li, Y.Q. Zha, T.D. Hu, Y.N. Xie, J. Zhang, J. Catal. 254 (2008) 310.
[38] M. Meng, Y.Q. Zha, J.Y. Luo, T.D. Hu, Y.N. Xie, T. Liu, J. Zhang, Appl. Catal. A 301 (2006) 145.
[39] O.V. Komova, A.V. Simakov, V.A. Rogov, D.I. Kochubei, G.V. Odegova, V.V. Kriventsov, E.A. Paukshtis, V.A. Ushakov, N.N. Sazonova, T.A. Nikoro, J. Mol. Catal. A 161 (2000) 191.
[40] J.R. Chang, S.L. Chang, T.B. Lin, J. Catal. 169 (1997) 338.
[41] L. Chmielarz, P. Kuśtrowski, A. Rafalska Łasocha, R. Dziembaj, Thermochim. Acta 395 (2003) 225.
[42] Z.P. Xu, H.C. Zeng, J. Phys. Chem. B 104 (2000) 10206.
[43] P. Arnoldy, J.A. Moulijn, J. Catal. 93 (1985) 38.
[44] S.J. Jelles, B. van Setten, M. Makkee, J.A. Moulijn, Appl. Catal. B: Environ. 21 (1999) 35.
[45] C. Janiak, R. Hoffmann, P. Sjovall, B. Kasemo, Langmuir 9 (1993) 3427.
[46] W.S. Epling, L.E. Campbell, A. Yezerets, N.W. Currier, J.E. Parks II, Catal. Rev. 46 (2004) 163.
[47] J.Y. Luo, M. Meng, Y.Q. Zha, Y.N. Xie, T.D. Hou, J. Zhang, T. Liu, Appl. Catal. B 78 (2008) 38.
[48] J.Y. Luo, M. Meng, X.G. Li, Y.Q. Zha, Micropor. Mesopor. Mater. 113 (2008) 277.
[49] K.I. Hadjiivanov, Catal. Rev. 42 (2000) 71.
[50] Y. Liu, M. Meng, X.G. Li, L.H. Guo, Y.Q. Zha, Chem. Eng. Res. Des. 86 (2008) 932.
[51] Y. Liu, M. Meng, Z.Q. Zou, X.G. Li, Y.Q. Zha, Catal. Commun. 10 (2008) 173.
[52] Ch. Sedlmair, K. Seshan, A. Jentys, J.A. Lercher, J. Catal. 214 (2003) 308.
[53] I. Perdana, D. Creaser, O. Öhrman, J. Hedlund, J. Catal. 234 (2005) 219.
[54] M. Meng, P.Y. Lin, Y.L. Fu, Catal. Lett. 48 (1997) 213.